

Theoretical study on the production of neutron-rich transuranium nuclei with radioactive beams in multinucleon transfer reactions

Jing-Jing Li,^{1,2} Na Tang,² Yu-Hai Zhang,² Xin-Rui Zhang,³ Gen Zhang,⁴ and Feng-Shou Zhang^{④,2,1,5,*}

¹Key Laboratory of Beam Technology of Ministry of Education, Institute of Radiation Technology, Beijing Academy of Science and Technology, Beijing 100875, China

²Key Laboratory of Beam Technology of Ministry of Education, College of Nuclear Science and Technology, Beijing Normal University, Beijing 100875, China

³Department of Physics, Guangxi Normal University, Guilin 541004, China

⁴School of Physical Science and Technology, Guangxi University, Nanning 530004, China

⁵Center of Theoretical Nuclear Physics, National Laboratory of Heavy Ion Accelerator of Lanzhou, Lanzhou 730000, China



(Received 28 April 2022; revised 6 June 2022; accepted 24 June 2022; published 11 July 2022)

The production of neutron-rich transuranium nuclei with $Z = 93\text{--}98$ in multinucleon transfer reactions induced by radioactive beams ^{92}Kr , ^{132}Sn , and ^{144}Xe with actinide target ^{238}U is investigated within the dinuclear system model with decay code GEMINI++. The isotopic distributions for reactions $^{136}\text{Xe} + ^{248}\text{Cm}$ and $^{136}\text{Xe} + ^{249}\text{Cf}$ are calculated and compared with the available experimental data. Theoretical calculations can reproduce the experimental results well. Both the N/Z ratio equilibration mechanism and driving potential dominate the transfer process of nucleons. Reaction $^{132}\text{Sn} + ^{238}\text{U}$ is an optimal projectile-target combination to obtain large production cross sections of neutron-rich isotopes with $Z = 93\text{--}98$. The corresponding optimal incident energy is also explored. The production cross sections of 41 unknown neutron-rich transuranium isotopes with cross sections greater than 1 nb are predicted. The reaction $^{132}\text{Sn} + ^{238}\text{U}$ at $E_{\text{c.m.}} = 521.3$ MeV shows huge advantages in producing neutron-rich transuranium nuclei with $Z = 93\text{--}98$.

DOI: [10.1103/PhysRevC.106.014606](https://doi.org/10.1103/PhysRevC.106.014606)

I. INTRODUCTION

Production of undiscovered neutron-rich nuclei far away from the β stability line in the heavy mass region is one of the frontiers in modern nuclear physics. Although 3327 nuclides have been discovered experimentally up to date [1], they are still far from the theoretical prediction of about 8000–10000 [2,3]. The vast unexplored area is located on the neutron-rich side in the northeast region of the nuclide chart. Synthesis of these unknown nuclides is important for understanding the nucleosynthesis in nuclear astrophysics and solving the puzzle of the origin of the heavy elements from iron to uranium in the universe.

Over the last decade, a large number of medium-mass neutron-rich nuclides have been produced by fission and projectile fragmentation reactions [4–12]. For example, at the RIKEN Nishina Center RI Beam Factory, 29 new neutron-rich isotopes in the rare-earth region were observed by the fission of 345 MeV/nucleon ^{238}U [6]. At GSI, 60 new neutron-rich isotopes in the atomic number range of $60 \leq Z \leq 78$ have been identified in fragmentation reactions with a 1 GeV/nucleon ^{238}U beam impinging on a Be target [8]. However, it seems that it is inaccessible to reach the region of transuranium neutron-rich nuclides by such types of reaction. Alternatively, multinucleon transfer (MNT) reaction becomes

a promising pathway to generate unknown neutron-rich nuclides in this region at present.

In the 1970s to 1990s, heavy-ion transfer reactions with actinide targets were widely investigated in experiments aiming to produce new neutron-rich actinide nuclides [13–25]. Neutron-rich actinide targets were bombarded with heavy projectiles, for example, the interactions of ^{86}Kr , ^{136}Xe , and ^{238}U with ^{248}Cm [21,23,24], ^{249}Cf [25], and so on. With the goal to produce neutron-rich nuclei along $N = 126$ as well as in the superheavy region, the MNT reactions attract renewed interest in recent years and much progress has been achieved [26–38]. Motivated by the attempt to populate neutron-rich isotopes around $N = 126$, the experimental research on MNT reaction $^{136}\text{Xe} + ^{198}\text{Pt}$ was performed at GANIL [30]. A great advantage of production cross sections is found in the MNT reaction in comparison to the projectile fragmentation reaction mechanism. At GSI, the deep inelastic MNT reaction of $^{48}\text{Ca} + ^{248}\text{Cm}$ was carried out and five new neutron-deficient isotopes with $Z > 92$ were observed [31].

Note that it is particularly difficult to produce unknown extremely neutron-rich heavy nuclides in MNT reactions with stable beams near the Coulomb barrier. Due to the larger neutron excess of neutron-rich radioactive beams, radioactive ion beams induced MNT reactions provide a possibility of generating new neutron-rich nuclides. With the development of new generations of radioactive beams facilities [39–43], several neutron-rich beams with high intensity would be provided in the near future. For instance, at the proposed intermediate

*Corresponding author: fszhang@bnu.edu.cn

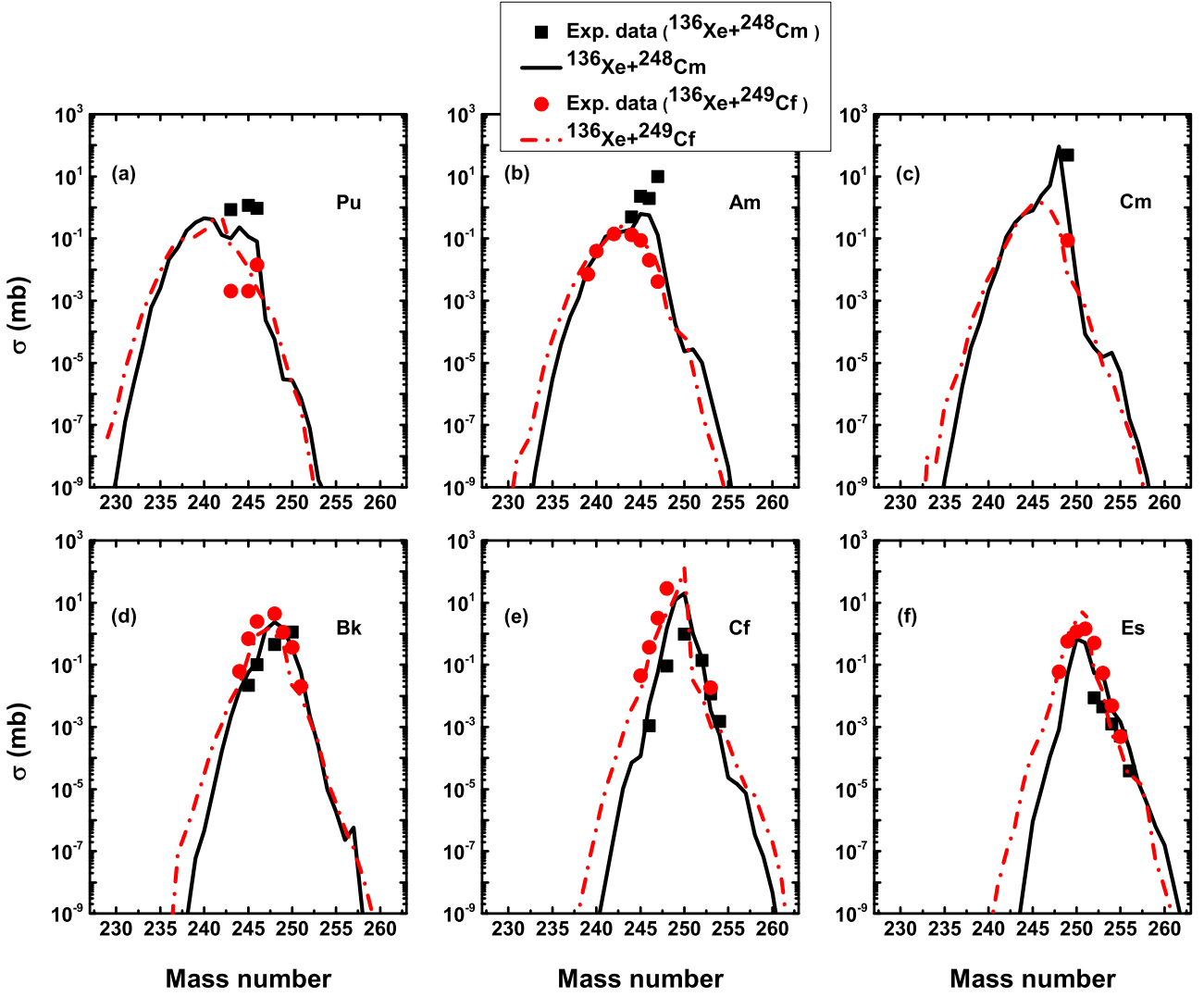


FIG. 1. The final isotopic production cross sections distributions of Pu, Am, Cm, Bk, Cf, and Es in MNT reactions $^{136}\text{Xe} + ^{248}\text{Cm}$ ($E_{\text{c.m.}} = 533$ MeV) and $^{136}\text{Xe} + ^{249}\text{Cf}$ ($E_{\text{c.m.}} = 526$ MeV). The black solid lines and red dashed lines denote the calculation results of $^{136}\text{Xe} + ^{248}\text{Cm}$ and $^{136}\text{Xe} + ^{249}\text{Cf}$, respectively. The experimental data taken from Refs. [24,25] are marked by black solid squares and red solid circles, respectively.

facility SPIRAL2 at GANIL [39], the intensities of the rare isotope beams in the mass range of 60–140 are expected to reach 10^6 – 10^{11} pps, such as 10^{10} pps for ^{92}Kr , 10^9 pps for ^{132}Sn and so on. Under this circumstances, MNT reactions induced by neutron-rich radioactive beams are expected to be a potential option of producing neutron-rich exotic nuclei.

A lot of theoretical models have been developed to study the MNT reactions near the Coulomb barrier. The phenomenological models, such as multidimensional Langevin-type dynamical equations of motion [44–47], dinuclear system (DNS) model [48–60], are widely used to investigate the dynamics of heavy ion damped collisions and the production of unknown heavy and superheavy neutron-rich nuclei. The GRAZING model describes the transfer of a few nucleon well [61–63]. The microscopic dynamics models, such as the time-dependent Hartree-Fock (TDHF) model [64–69]

and improved quantum molecular dynamics (ImQMD) model [70–74], are successfully applied to the MNT reactions in low-energy heavy-ion collisions. More comprehensive reviews see Refs. [75–81].

In this work, the transfer reactions induced by neutron-rich radioactive beams ^{92}Kr , ^{132}Sn , and ^{144}Xe with actinide target ^{238}U are investigated based on the DNS model with GEMINI++ code. The effects of N/Z ratio equilibration mechanism and driving potential on the transfer of nucleons are analyzed. The incident energy dependence on the production of neutron-rich transuranium nuclei is also studied. The production cross sections of unknown neutron-rich transuranium isotopes with $Z = 93$ – 98 in reaction $^{132}\text{Sn} + ^{238}\text{U}$ are predicted.

This paper is organized as follows. In Sec. II, a brief description of the DNS model is given. The optimal projectile-target combination and incident energy to produce

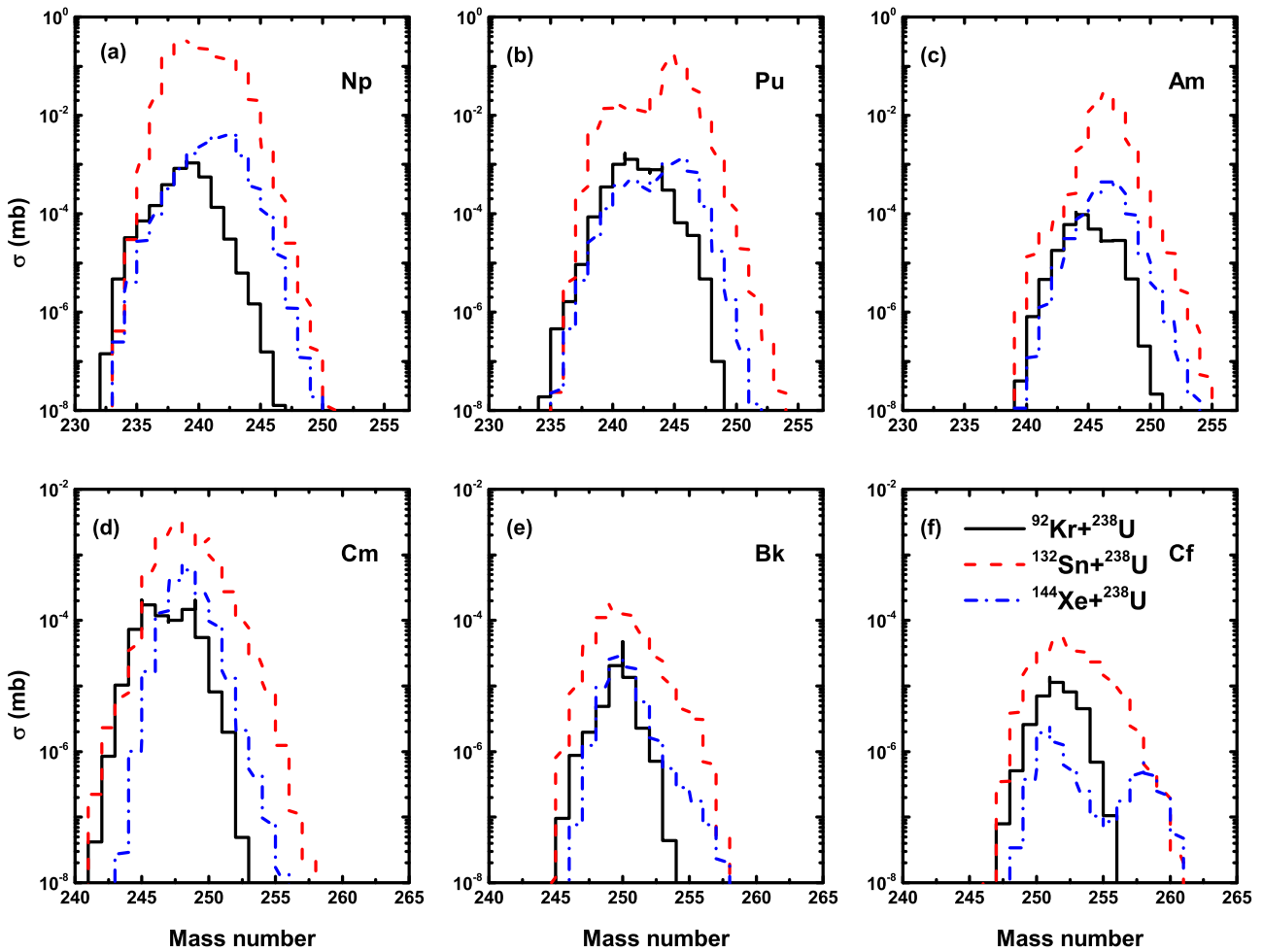


FIG. 2. The final isotopic production cross section distributions of Np, Pu, Am, Cm, Bk, and Cf in MNT reactions $^{92}\text{Kr} + ^{238}\text{U}$ (black solid lines), $^{132}\text{Sn} + ^{238}\text{U}$ (red dashed lines), and $^{144}\text{Xe} + ^{238}\text{U}$ (blue dash-dotted lines) at $E_{\text{c.m.}} = 1.10 V_B$.

neutron-rich nuclei with $Z = 93\text{--}98$ are discussed in Sec. III. Finally, a summary is presented in Sec. IV.

II. THEORETICAL MODEL

Within the framework of the DNS model, the nucleon transfer at the contact configuration of two colliding nuclei is determined by the potential energy surface (PES). The PES of a reaction system is defined as [82]

$$U(Z_1, N_1, Z_2, N_2, R_{\text{cont}}) = \Delta(Z_1, N_1) + \Delta(Z_2, N_2) + V_{\text{CN}}(Z_1, N_1, Z_2, N_2, R_{\text{cont}}, \theta_1, \theta_2). \quad (1)$$

Here, $\Delta(Z_1, N_1)$ and $\Delta(Z_2, N_2)$ are the mass excess of the fragment (Z_1, N_1) and (Z_2, N_2) , respectively, where the shell correction energy and the pair energy taken in Ref. [2] are also taken into consideration. V_{CN} denotes the nucleus-nucleus interaction potential energy, which is the sum of Coulomb interaction potential and nuclear potential. R_{cont} is the position where the nucleon transfer process takes place. We assume $R_{\text{cont}} = R_1[1 + \beta_1 Y_{20}(\theta_1)] + R_2[1 + \beta_2 Y_{20}(\theta_2)] +$

0.7 fm for heavy reaction system with no potential pocket. $R_{1,2} = 1.16 A_{1,2}^{1/3}$. β_1 and β_2 are the quadrupole deformation parameters of two fragments which are taken from Ref. [2]. $\theta_{1,2}$ is the angle between the collision axis and the symmetry axis of the deformed fragments.

The calculation of V_{CN} is written as

$$\begin{aligned} V_{\text{CN}}(Z_1, N_1, Z_2, N_2, R, \beta_1, \beta_2) &= V_{\text{C}}(Z_1, N_1, Z_2, N_2, R, \beta_1, \beta_2) \\ &\quad + V_{\text{N}}(Z_1, N_1, Z_2, N_2, R, \beta_1, \beta_2), \end{aligned} \quad (2)$$

where the Coulomb interaction potential V_{C} adopts Wong's formula [83] and the nuclear potential V_{N} is calculated by double folding potential [82]. More detailed descriptions see Ref. [60].

The nucleon transfer process between the DNS is considered as a diffusion process. The time evolution of the distribution probability $P(Z_1, N_1, E_1, t)$ for a fragment with proton number Z_1 , neutron number N_1 , and excitation energy E_1 is calculated by solving the following master

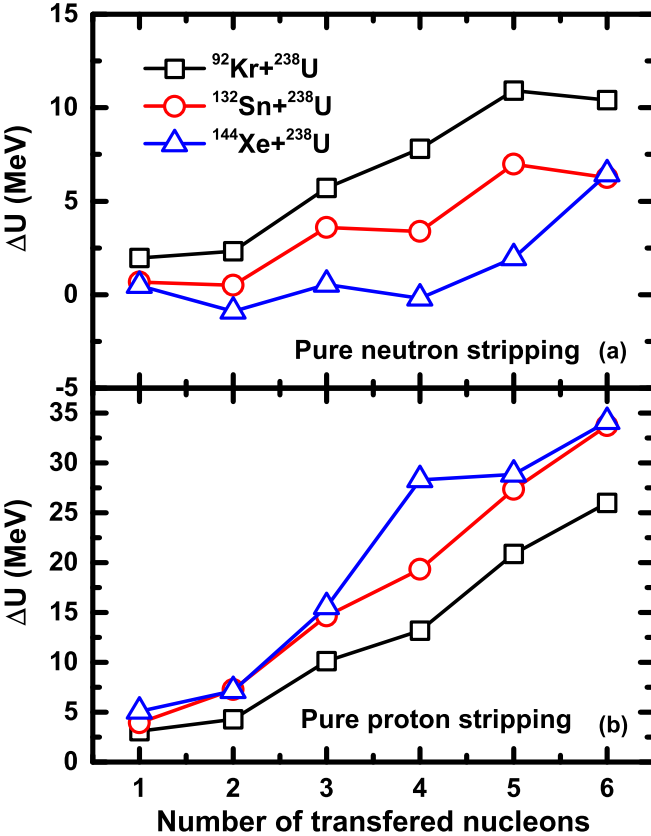


FIG. 3. The values of the driving potential which need to overcome (ΔU) during the transfer of nucleons as a function of the number of transferred nucleons in reactions $^{92}\text{Kr} + ^{238}\text{U}$, $^{132}\text{Sn} + ^{238}\text{U}$, and $^{144}\text{Xe} + ^{238}\text{U}$. (a) and (b) denote the pure neutron stripping channel and pure proton stripping channel, respectively.

equation [55,84]:

$$\begin{aligned} & \frac{dP(Z_1, N_1, E_1, t)}{dt} \\ &= \sum_{Z'_1} W_{Z_1, N_1; Z'_1, N_1}(t) [d_{Z_1, N_1} P(Z'_1, N_1, E'_1, t) \\ &\quad - d_{Z'_1, N_1} P(Z_1, N_1, E_1, t)] \\ &+ \sum_{N'_1} W_{Z_1, N_1; Z_1, N'_1}(t) [d_{Z_1, N_1} P(Z_1, N'_1, E'_1, t) \\ &\quad - d_{Z_1, N'_1} P(Z_1, N_1, E_1, t)]. \end{aligned} \quad (3)$$

The sum is taken over all possible proton and neutron numbers that fragment (Z'_1, N'_1) may take. $W_{Z_1, N_1; Z'_1, N_1}$ (or $W_{Z_1, N_1; Z_1, N'_1}$) is the mean transition probability from channel (Z_1, N_1, E_1) to (Z'_1, N_1, E'_1) [or from channel (Z_1, N_1, E_1) to (Z_1, N'_1, E'_1)]. d_{Z_1, N_1} denotes the microscopic dimensions corresponding to the macroscopic state (Z_1, N_1, E_1) . For a more detailed introduction of the mean transition probability and microscopic dimensions see Refs. [85,86]. The interaction time is calculated by using the deflection function method [87].

The excitation energy of the DNS is defined as

$$E_{\text{DNS}}^* = E_{\text{diss}} - [U(Z_1, N_1, Z_2, N_2) - U(Z_P, N_P, Z_T, N_T)] - \frac{M^2}{2\xi_{\text{int}}}. \quad (4)$$

E_{diss} is the energy dissipation from the incident energy to the DNS. $U(Z_1, N_1, Z_2, N_2)$ and $U(Z_P, N_P, Z_T, N_T)$ are the PES corresponding to the configuration of (Z_1, N_1, Z_2, N_2) and the entrance point (Z_P, N_P, Z_T, N_T) , respectively. M and ξ_{int} denote the intrinsic angular momentum of the DNS and the intrinsic moment of inertia, respectively. The calculation of E_{diss} , M and ξ_{int} see Ref. [86]. It is assumed that the excitation energy of primary fragments is proportional to its mass.

The production cross section of a primary fragment with charge number Z_1 and neutron number N_1 are calculated by

$$\sigma_{\text{pr}}^{\text{DNS}}(Z_1, N_1, E_{\text{c.m.}}) = \frac{\pi \hbar^2}{2\mu E_{\text{c.m.}}} \sum_J (2J + 1) \times [P(Z_1, N_1, E_1, t = \tau_{\text{int}})], \quad (5)$$

where μ and $E_{\text{c.m.}}$ are the reduced mass of the system and the incident energy at the center of mass frame, respectively. $P(Z_1, N_1, E_1)$ is the fragment distribution probability at time $t = \tau_{\text{int}}$. The code GEMINI++ is used to treat the de-excitation process of the primary excited fragments [88,89]. During the de-excitation process, emission of light particles and γ rays is in competition with the fission of fragments and each fragment is simulated 1000 times.

III. RESULTS AND DISCUSSION

A. Comparison with experimental data

In order to test the reliability of the theoretical model described above, the final production cross sections of transuranium isotopes in MNT reactions $^{136}\text{Xe} + ^{248}\text{Cm}$ and $^{136}\text{Xe} + ^{249}\text{Cf}$ at $E_{\text{c.m.}} = 533$ MeV and $E_{\text{c.m.}} = 526$ MeV are calculated. The comparison of the calculation results with the experimental data are shown in Fig. 1. The black solid squares and red solid circles represent the experimental data which are taken from Refs. [24,25]. The black solid lines and red dash-dotted lines denote the calculation results of $^{136}\text{Xe} + ^{248}\text{Cm}$ and $^{136}\text{Xe} + ^{249}\text{Cf}$, respectively. A good agreement between the experimental data and the calculation results can be observed from Fig. 1, especially for reaction $^{136}\text{Xe} + ^{249}\text{Cf}$.

Around the peak position, one can see that the measured final production cross sections of targetlike fragments (TLFs) for $Z = 94\text{--}96$ are larger in the reaction $^{136}\text{Xe} + ^{248}\text{Cm}$ than that in reaction $^{136}\text{Xe} + ^{249}\text{Cf}$. It is the opposite for isotopes with $Z = 97\text{--}99$. Our calculation results are consistent with the measured data. On the neutron-rich side, it is noticed that the predicted production cross sections of all TLFs are larger in the reaction $^{136}\text{Xe} + ^{248}\text{Cm}$, with the exception of Cf isotopes. The phenomenon is the opposite on the neutron-deficient side. This is attributed to the different N/Z ratio of target. The N/Z ratio of ^{249}Cf is 1.541, which is much smaller than that of ^{248}Cm ($N/Z = 1.583$). The detail interpretation is stated in Ref. [86].

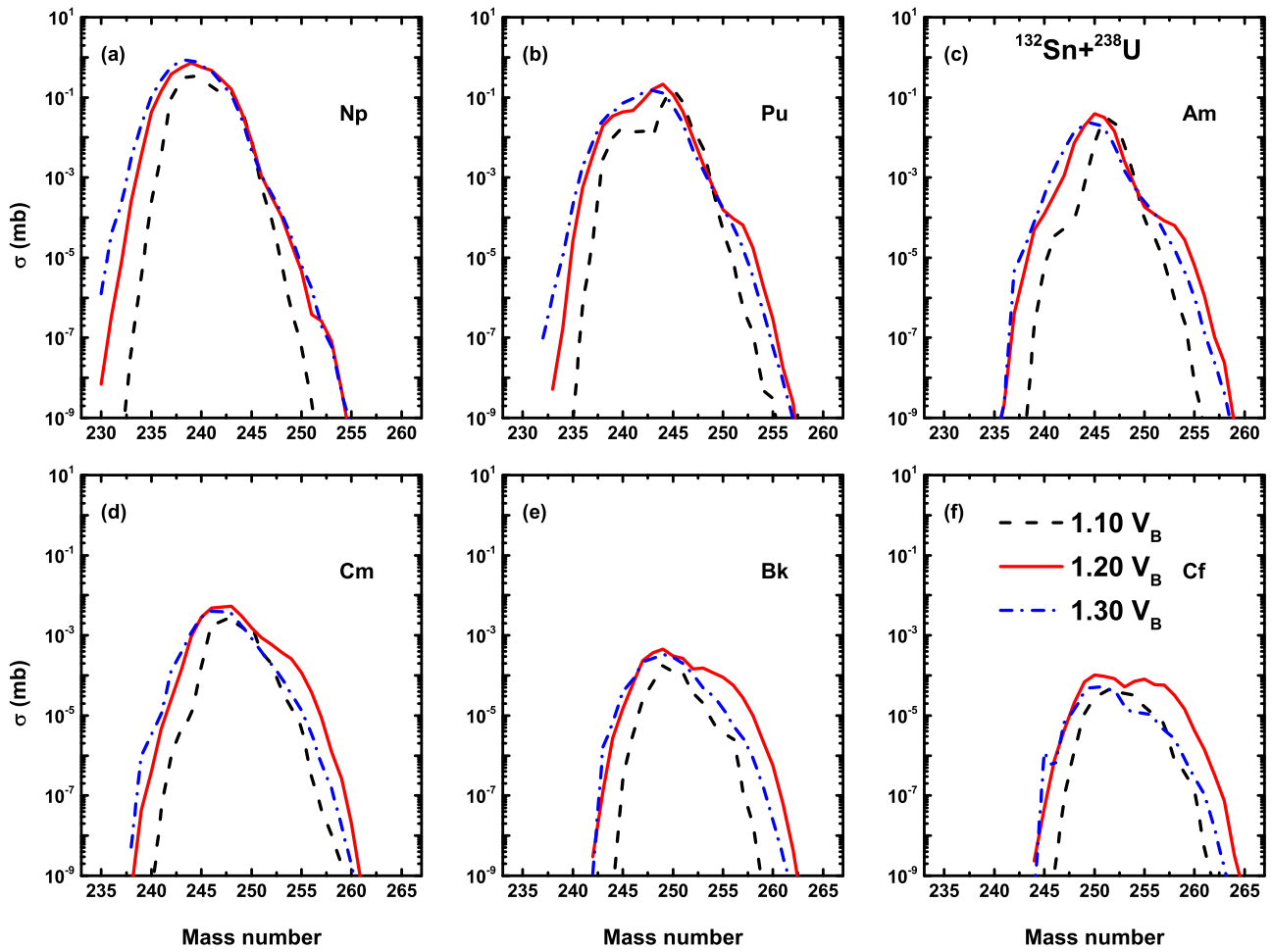


FIG. 4. The final isotopic production cross section distributions of Np, Pu, Am, Cm, Bk, and Cf in the $^{132}\text{Sn} + ^{238}\text{U}$ reaction at $E_{\text{c.m.}} = 1.10 V_B$, $1.20 V_B$, and $1.30 V_B$, respectively. The dashed, solid, and dash-dotted lines indicate different incident energies.

B. The suitable projectile-target combination and incident energy to obtain large production cross sections of neutron-rich nuclei with $Z = 93\text{--}98$

Experimental and theoretical research have revealed that the distributions of transfer products in the reaction system with more neutrons tend to be on the neutron-rich side. The neutron-rich radioactive beams generally feature larger neutron excess, leading to the production of more neutron-rich nuclei. In Ref. [39], the author pointed out that the after acceleration intensities of radioactive beams ^{92}Kr , ^{132}Sn , and ^{144}Xe should reach 10^{10} pps, 10^9 pps and 5×10^8 pps, respectively. In this section, we investigate the production of neutron-rich transuranium nuclei with $Z = 93\text{--}98$ in MNT reactions induced by neutron-rich radioactive beams ^{92}Kr , ^{132}Sn , and ^{144}Xe with actinide target ^{238}U . In order to search for the optimal projectile-target combination, we first calculate the production cross section distributions of TLFs in ^{92}Kr , ^{132}Sn , and ^{144}Xe induced ^{238}U -based MNT reactions at $E_{\text{c.m.}} = 1.10 V_B$, as shown in Fig. 2. Here, V_B is the Bass interaction barrier [90]. The black solid lines, red dashed lines, and blue dash-dotted lines denote the different reactions. The V_B values for the three reactions are 324.5 MeV, 434.4 MeV, and 464.8 MeV, respectively. On the neutron-rich side, it is obvious to

observe that the isotopic production cross sections in reactions $^{132}\text{Sn} + ^{238}\text{U}$ and $^{144}\text{Xe} + ^{238}\text{U}$ are much larger than that in reaction $^{92}\text{Kr} + ^{238}\text{U}$. One important reason is the effect of N/Z ratio equilibration. The N/Z ratios of ^{132}Sn and ^{144}Xe are 1.640 and 1.666, which are significantly larger than that of ^{238}U (1.586). Dominated by the N/Z ratio equilibrium mechanism, it is easier for target ^{238}U to obtain neutrons from projectiles. Whereas the N/Z ratio of ^{92}Kr is 1.551, which is much smaller than that of ^{238}U , hence it is quite difficult for ^{92}Kr to transfer neutrons to ^{238}U .

In order to demonstrate the transfer of nucleons quantitatively, the value of the driving potential which need to be overcome (ΔU) during the transfer of nucleons is extracted. We defined the ΔU as $\Delta U = U(Z_1, N_1, Z_2, N_2) - U(Z_P, N_P, Z_T, N_T)$. The values of ΔU as a function of the number of transferred nucleons in reactions $^{92}\text{Kr} + ^{238}\text{U}$, $^{132}\text{Sn} + ^{238}\text{U}$, and $^{144}\text{Xe} + ^{238}\text{U}$ are shown in Fig. 3. Figure 3(a) denotes the pure neutron stripping channel. It can be seen that the lower potential needs to be overcome in reaction $^{144}\text{Xe} + ^{238}\text{U}$ in the case of stripping one to five neutrons. Thus ^{238}U more easily gains one to five neutrons from ^{144}Xe . But the values of ΔU in reaction $^{132}\text{Sn} + ^{238}\text{U}$ are slightly lower than that in reaction $^{144}\text{Xe} + ^{238}\text{U}$ when six neutrons

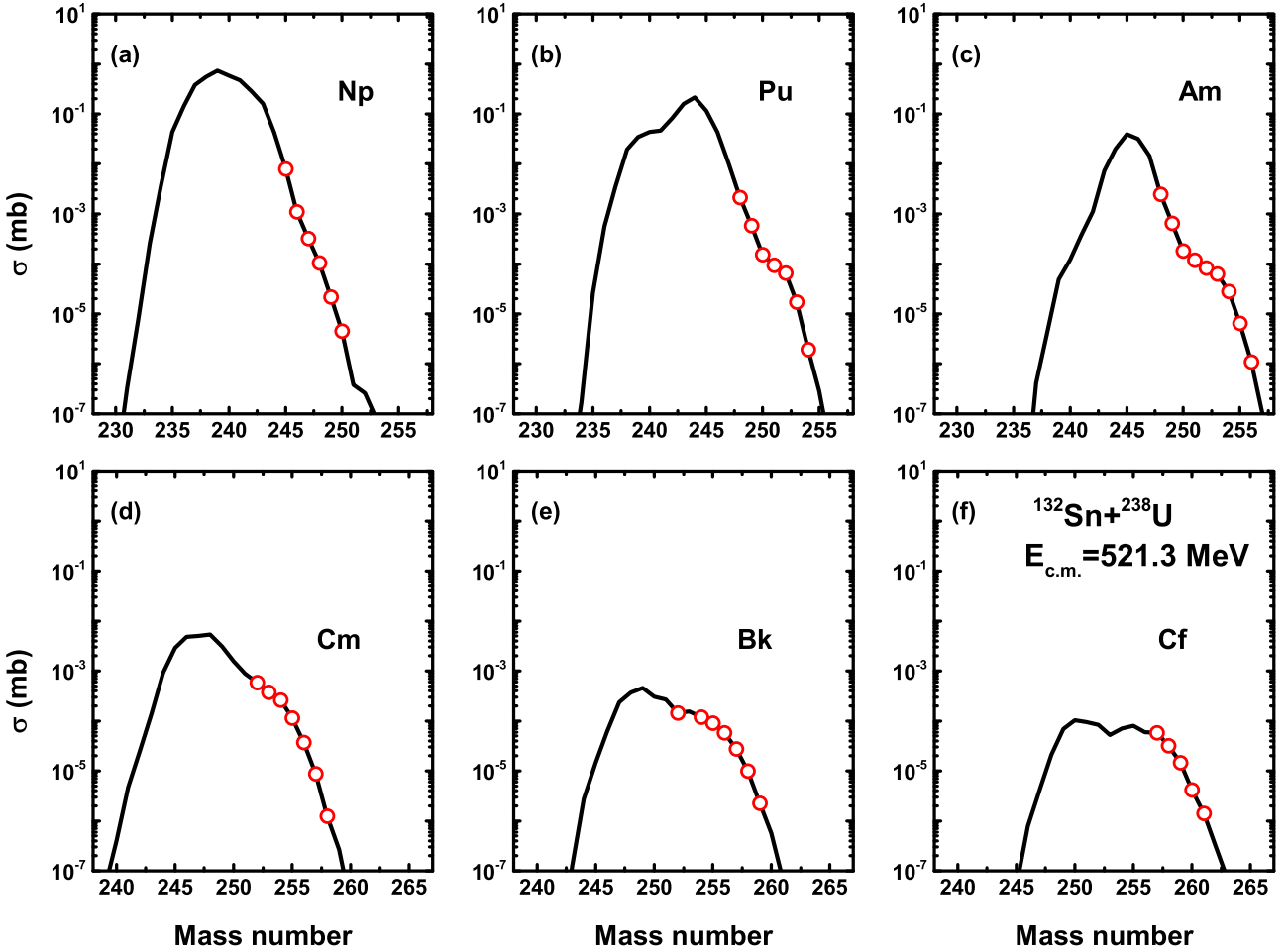


FIG. 5. The production cross sections of TLFs with $Z = 93\text{--}98$ for reaction $^{132}\text{Sn} + ^{238}\text{U}$ at $E_{\text{c.m.}} = 521.3$ MeV. The empty circles denote the unknown neutron-rich nuclei with cross sections greater than 1 nb.

are stripped from the projectile. The pure proton stripping channel is displayed in Fig. 3(b). One can find that with an increasing number of stripping protons, more potential energy needs to be overcome. The values of ΔU in $^{144}\text{Xe} + ^{238}\text{U}$ are the largest when one to six protons are stripped from the projectile, which leads to a suppression in the formation probabilities of transuranium nuclei in $^{144}\text{Xe} + ^{238}\text{U}$. Dominated by a combination of N/Z ratio equilibration mechanism and driving potential, $^{132}\text{Sn} + ^{238}\text{U}$ is a preferable combination for the production of neutron-rich transuranium isotopes with $Z = 93\text{--}98$.

The transfer cross sections strongly depend on the incident energy in low energy MNT reactions. Exploring an optimal incident energy provides important guidance for experiments. The influence of incident energy on the transfer cross sections in reaction $^{132}\text{Sn} + ^{238}\text{U}$ is analyzed. In Fig. 4, the calculated final isotopic production cross sections of Np, Pu, Am, Cm, Bk, and Cf in reaction $^{132}\text{Sn} + ^{238}\text{U}$ at $E_{\text{c.m.}} = 1.10 V_B$, $1.20 V_B$, and $1.30 V_B$ are displayed. The dashed, solid, and dash-dotted lines indicate different incident energies. One can see that the production cross sections are relatively low at $E_{\text{c.m.}} = 1.10 V_B$. A weaker energy dependence is observed at $E_{\text{c.m.}} = 1.20 V_B\text{--}1.30 V_B$ on the neutron-deficient side.

However, on the neutron-rich side, the dependence of production cross section distributions for TLFs on incident energy becomes stronger with the increase of the charge number. It is found that the production cross sections of neutron-rich isotopes at $1.20 V_B$ are slightly larger than those at $1.30 V_B$. One important reason is that the fission probability becomes more significant at higher excitation energy, leading to a depression of primary fragment survival. For example, at the central collisions, the excitation energy of neutron-rich ^{254}Bk is 38.670 MeV at $E_{\text{c.m.}} = 1.20 V_B$, which is lower than that (47.771 MeV) at $E_{\text{c.m.}} = 1.30 V_B$. We can conclude that $E_{\text{c.m.}} = 1.20 V_B$ (521.3 MeV) is the optimal incident energy for production neutron-rich transuranium isotopes with $Z = 93\text{--}98$ in MNT reaction $^{132}\text{Sn} + ^{238}\text{U}$.

The influence of the incident energy on production cross sections of TLFs with $Z = 93\text{--}98$ in reactions $^{92}\text{Kr} + ^{238}\text{U}$ and $^{144}\text{Xe} + ^{238}\text{U}$ is also studied. The general trends are similar. In the $^{144}\text{Xe} + ^{238}\text{U}$ collision, the optimal incident energy is $1.20 V_B$ (557.8 MeV), which is the same with the reaction $^{132}\text{Sn} + ^{238}\text{U}$. But the corresponding optimal incident energy is $1.30 V_B$ for reaction $^{92}\text{Kr} + ^{238}\text{U}$, which is 421.7 MeV. This is attributed to the differences of interaction barriers. The Bass interaction barriers in reactions $^{132}\text{Sn} + ^{238}\text{U}$ and

$^{144}\text{Xe} + ^{238}\text{U}$ are 434.4 MeV and 464.8 MeV, respectively. However, the Bass interaction barrier is much lower in reaction $^{92}\text{Kr} + ^{238}\text{U}$, which is 324.5 MeV.

C. Production cross sections of unknown neutron-rich transuranium isotopes with $Z = 93\text{--}98$

Prediction the production cross sections of new nuclei provides important guidance for performing future experiment. According to the discussion in the last subsection, reaction $^{132}\text{Sn} + ^{238}\text{U}$ is an optimal combination for producing neutron-rich transuranium isotopes with $Z = 93\text{--}98$, and the corresponding optimal incident energy is 521.3 MeV. Figure 5 shows the production cross sections of final TLFs with $Z = 93\text{--}98$ in the MNT reaction $^{132}\text{Sn} + ^{238}\text{U}$ at $E_{\text{c.m.}} = 521.3$ MeV. The empty circles denote the unknown neutron-rich nuclei with cross sections greater than 1 nb. It can be found that with the increasing charge number of TLFs, the production cross sections of transuranium isotopes decrease rapidly. The reason is that higher potential energy needs to be overcome when more protons are transferred from ^{132}Sn to ^{238}U , leading to the suppression of cross sections.

From Fig. 5, one can see that a total of 41 unknown neutron-rich nuclei would expect to be produced with cross sections greater than 1 nb, filling the gap in the region of transuranium. The predicted production cross sections of $^{245,246,247,248,249}\text{Np}$ are $8.03 \mu\text{b}$, $1.12 \mu\text{b}$, $0.33 \mu\text{b}$, $0.11 \mu\text{b}$, and $0.02 \mu\text{b}$, respectively. For $^{248,249,250,251,252,253}\text{Pu}$, they are $2.15 \mu\text{b}$, $0.59 \mu\text{b}$, $0.16 \mu\text{b}$, $0.09 \mu\text{b}$, $0.06 \mu\text{b}$, and $0.02 \mu\text{b}$, respectively. The calculated production cross sections of $^{248,249,250,251,252,253,254}\text{Am}$ are $2.47 \mu\text{b}$, $0.65 \mu\text{b}$, $0.18 \mu\text{b}$, $0.12 \mu\text{b}$, $0.08 \mu\text{b}$, $0.06 \mu\text{b}$, and $0.02 \mu\text{b}$, respectively. $^{252,253,254,255,256}\text{Cm}$ are $0.59 \mu\text{b}$, $0.37 \mu\text{b}$, $0.26 \mu\text{b}$, $0.12 \mu\text{b}$, and $0.04 \mu\text{b}$, respectively. $^{252,254,255,256,257}\text{Bk}$ are $0.15 \mu\text{b}$, $0.12 \mu\text{b}$, $0.09 \mu\text{b}$, $0.06 \mu\text{b}$, and $0.03 \mu\text{b}$, respectively. The production cross sections of $^{257,258,259}\text{Cf}$ are $0.06 \mu\text{b}$, $0.03 \mu\text{b}$, and $0.01 \mu\text{b}$, respectively. We can conclude

that reaction $^{132}\text{Sn} + ^{238}\text{U}$ at $E_{\text{c.m.}} = 521.3$ MeV is a promising candidate to produce neutron-rich transuranium isotopes with $Z = 93\text{--}98$.

IV. SUMMARY

The MNT reactions $^{136}\text{Xe} + ^{248}\text{Cm}$, $^{136}\text{Xe} + ^{249}\text{Cf}$, $^{92}\text{Kr} + ^{238}\text{U}$, $^{132}\text{Sn} + ^{238}\text{U}$, and $^{144}\text{Xe} + ^{238}\text{U}$ are investigated by using the DNS model combined with the GEMINI++ code. Our calculation results can reproduce the available experimental data well for reactions $^{136}\text{Xe} + ^{248}\text{Cm}$ and $^{136}\text{Xe} + ^{249}\text{Cf}$. The distributions of TLFs in MNT reactions induced by radioactive beams ^{92}Kr , ^{132}Sn , and ^{144}Xe with actinide target ^{238}U are analyzed. It is found that the transfer of nucleons are dominated by the N/Z ratio equilibration and driving potential. The effect of incident energy on production cross sections in these three reactions is also studied. Due to the influence of the interaction barrier, 1.20 V_B is the optimal incident energy to produce neutron-rich transuranium isotopes with $Z = 93\text{--}98$ for reactions $^{132}\text{Sn} + ^{238}\text{U}$ and $^{144}\text{Xe} + ^{238}\text{U}$. But the optimal incident energy is around 1.30 V_B for reaction $^{92}\text{Kr} + ^{238}\text{U}$. The combination of ^{132}Sn with ^{238}U is a suitable reaction partner to gain large production cross sections of neutron-rich transuranium nuclei. The production cross sections of 41 new neutron-rich transuranium isotopes with $Z = 93\text{--}98$ are predicted in reaction $^{132}\text{Sn} + ^{238}\text{U}$. This study indicates that reaction $^{132}\text{Sn} + ^{238}\text{U}$ at $E_{\text{c.m.}} = 521.3$ MeV shows great advantages in producing neutron-rich transuranium isotopes with $Z = 93\text{--}98$.

ACKNOWLEDGMENTS

This work was supported by the National Natural Science Foundation of China under Grants No. 12105019, 12047513, 12135004, 11635003, 11961141004; the Beijing Postdoctoral Research Foundation (2021-zz-089); the Guangxi Science and Technology Base and Special Talent Program under Grant No. 2021AC19266.

-
- [1] M. Thoennessen, Discovery of Nuclides Project, <https://people.nscl.msu.edu/~thoennes/isotopes> (2022).
 - [2] P. Moller, J. Nix, W. Myers, and W. Swiatecki, *At. Data Nucl. Data Tables* **59**, 185 (1995).
 - [3] J. Erler, N. Birge, M. Kortelainen, W. Nazarewicz, E. Olsen, A. M. Perhac, and M. Stoitsov, *Nature (London)* **486**, 509 (2012).
 - [4] T. Ohnishi, T. Kubo, K. Kusaka, A. Yoshida, K. Yoshida, M. Ohtake, N. Fukuda, H. Takeda, D. Kameda, K. Tanaka, N. Inabe, Y. Yanagisawa, Y. Gono, H. Watanabe, H. Otsu, H. Baba, T. Ichihara, Y. Yamaguchi, M. Takechi, S. Nishimura *et al.*, *J. Phys. Soc. Jpn.* **79**, 073201 (2010).
 - [5] Y. Shimizu, T. Kubo, N. Fukuda, N. Inabe, D. Kameda, H. Sato, H. Suzuki, H. Takeda, K. Yoshida, and G. Lorusso, *J. Phys. Soc. Jpn.* **87**, 014203 (2018).
 - [6] N. Fukuda, T. Kubo, D. Kameda, N. Inabe, H. Suzuki, Y. Shimizu, H. Takeda, K. Kusaka, Y. Yanagisawa, and M. Ohtake, *J. Phys. Soc. Jpn.* **87**, 014202 (2018).
 - [7] H. Alvarez-Pol, J. Benlliure, E. Casarejos, L. Audouin, D. Cortina-Gil, T. Enqvist, B. Fernández-Domínguez, A. R. Junghans, B. Jurado, P. Napolitani, J. Pereira, F. Rejmund, K.-H. Schmidt, and O. Yordanov, *Phys. Rev. C* **82**, 041602(R) (2010).
 - [8] J. Kurcewicz, F. Farinon, H. Geissel, S. Pietri, C. Nociforo, A. Prochazka, H. Weick, J. Winfield, A. Estradé, P. Allegro, A. Bail, G. Bélier, J. Benlliure, G. Benzoni, M. Bunce, M. Bowry, R. Caballero-Folch, I. Dillmann, A. Evdokimov, J. Gerl *et al.*, *Phys. Lett. B* **717**, 371 (2012).
 - [9] I. Mukha, L. V. Grigorenko, X. Xu, L. Acosta, E. Casarejos, A. A. Ciemny, W. Dominik, J. Duénas-Díaz, V. Dunin, J. M. Espino, A. Estradé, F. Farinon, A. Fomichev, H. Geissel, T. A. Golubkova, A. Gorshkov, Z. Janas, G. Kamiński, O. Kiselev, R. Knöbel *et al.*, *Phys. Rev. Lett.* **115**, 202501 (2015).
 - [10] O. B. Tarasov, M. Portillo, D. J. Morrissey, A. M. Amthor, L. Bandura, T. Baumann, D. Bazin, J. S. Berryman, B. A. Brown, G. Chubarian, N. Fukuda, A. Gade, T. N. Ginter, M. Hausmann,

- N. Inabe, T. Kubo, J. Pereira, B. M. Sherrill, A. Stolz, C. Sumithrarachchi *et al.*, *Phys. Rev. C* **87**, 054612 (2013).
- [11] A. A. Ciemny, W. Dominik, T. Ginter, R. Grzywacz, Z. Janas, M. Kuich, C. Mazzocchi, M. Pfützner, M. Pomorski, F. Zarzyński, D. Bazin, T. Baumann, A. Bezbakh, B. P. Crider, M. Ćwiok, S. Go, G. Kamiński, K. Kolos, A. Korgul, E. Kwan *et al.*, *Phys. Rev. C* **92**, 014622 (2015).
- [12] R. Ogul, A. S. Botvina, U. Atav, N. Buyukcizmeci, I. N. Mishustin, P. Adrich, T. Aumann, C. O. Bacri, T. Barczyk, R. Bassini, S. Bianchin, C. Boiano, A. Boudard, J. Brzychczyk, A. Chbihi, J. Cibor, B. Czech, M. De Napoli, J.-E. Ducret, H. Emling *et al.*, *Phys. Rev. C* **83**, 024608 (2011).
- [13] J. V. Kratz, A. E. Norris, and G. T. Seaborg, *Phys. Rev. Lett.* **33**, 502 (1974).
- [14] R. J. Otto, M. M. Fowler, D. Lee, and G. T. Seaborg, *Phys. Rev. Lett.* **36**, 135 (1976).
- [15] J. V. Kratz, J. O. Liljenzin, A. E. Norris, and G. T. Seaborg, *Phys. Rev. C* **13**, 2347 (1976).
- [16] U. Reus, A. M. Habbestad Wätzig, R. A. Esterlund, P. Patzelt, and I. S. Grant, *Phys. Rev. Lett.* **39**, 171 (1977).
- [17] E. K. Hulet, R. W. Lougheed, J. F. Wild, J. H. Landrum, P. C. Stevenson, A. Ghiorso, J. M. Nitschke, R. J. Otto, D. J. Morrissey, P. A. Baisden, B. F. Gavin, D. Lee, R. J. Silva, M. M. Fowler, and G. T. Seaborg, *Phys. Rev. Lett.* **39**, 385 (1977).
- [18] M. Schädel, J. V. Kratz, H. Ahrens, W. Brüchle, G. Franz, H. Gäggeler, I. Warnecke, G. Wirth, G. Herrmann, N. Trautmann, and M. Weis, *Phys. Rev. Lett.* **41**, 469 (1978).
- [19] P. Glässel, D. v. Harrach, Y. Civelekoglu, R. Männer, H. J. Specht, J. B. Wilhelmy, H. Freiesleben, and K. D. Hildenbrand, *Phys. Rev. Lett.* **43**, 1483 (1979).
- [20] D. Lee, H. von Gunten, B. Jacak, M. Nurmia, Y.-F. Liu, C. Luo, G. T. Seaborg, and D. C. Hoffman, *Phys. Rev. C* **25**, 286 (1982).
- [21] M. Schädel, W. Brüchle, H. Gäggeler, J. V. Kratz, K. Sümmerer, G. Wirth, G. Herrmann, R. Stakemann, G. Tittel, N. Trautmann, J. M. Nitschke, E. K. Hulet, R. W. Lougheed, R. L. Hahn, and R. L. Ferguson, *Phys. Rev. Lett.* **48**, 852 (1982).
- [22] D. Lee, K. J. Moody, M. J. Nurmia, G. T. Seaborg, H. R. von Gunten, and D. C. Hoffman, *Phys. Rev. C* **27**, 2656 (1983).
- [23] K. J. Moody, D. Lee, R. B. Welch, K. E. Gregorich, G. T. Seaborg, R. W. Lougheed, and E. K. Hulet, *Phys. Rev. C* **33**, 1315 (1986).
- [24] R. B. Welch, K. J. Moody, K. E. Gregorich, D. Lee, and G. T. Seaborg, *Phys. Rev. C* **35**, 204 (1987).
- [25] K. E. Gregorich, K. J. Moody, D. Lee, W. K. Kot, R. B. Welch, P. A. Wilmarth, and G. T. Seaborg, *Phys. Rev. C* **35**, 2117 (1987).
- [26] E. M. Kozulin, E. Vardaci, G. N. Knyazheva, A. A. Bogachev, S. N. Dmitriev, I. M. Itkis, M. G. Itkis, A. G. Knyazev, T. A. Loktev, K. V. Novikov, E. A. Razinkov, O. V. Rudakov, S. V. Smirnov, W. Trzaska, and V. I. Zagrebaev, *Phys. Rev. C* **86**, 044611 (2012).
- [27] J. V. Kratz, M. Schädel, and H. W. Gäggeler, *Phys. Rev. C* **88**, 054615 (2013).
- [28] O. Beliuskina, S. Heinz, V. Zagrebaev, V. Comas, C. Heinz, S. Hofmann, R. KnöBel, M. Stahl, D. Ackermann, and F. P. Heßberger, *Eur. Phys. J. A* **50**, 1 (2014).
- [29] J. S. Barrett, W. Loveland, R. Yanez, S. Zhu, A. D. Ayangeakaa, M. P. Carpenter, J. P. Greene, R. V. F. Janssens, T. Lauritsen, E. A. McCutchan, A. A. Sonzogni, C. J. Chiara, J. L. Harker, and W. B. Walters, *Phys. Rev. C* **91**, 064615 (2015).
- [30] Y. X. Watanabe, Y. H. Kim, S. C. Jeong, Y. Hirayama, N. Imai, H. Ishiyama, H. S. Jung, H. Miyatake, S. Choi, J. S. Song, E. Clement, G. de France, A. Navin, M. Rejmund, C. Schmitt, G. Pollaro, L. Corradi, E. Fioretto, D. Montanari, M. Niikura *et al.*, *Phys. Rev. Lett.* **115**, 172503 (2015).
- [31] H. Devaraja, S. Heinz, O. Beliuskina, V. Comas, S. Hofmann, C. Hornung, G. Münzenberg, K. Nishio, D. Ackermann, Y. Gambhir, M. Gupta, R. Henderson, F. Heßberger, J. Khuyagbaatar, B. Kindler, B. Lommel, K. Moody, J. Maurer, R. Mann, A. Popeko *et al.*, *Phys. Lett. B* **748**, 199 (2015).
- [32] A. Vogt, B. Birkenbach, P. Reiter, L. Corradi, T. Mijatović, D. Montanari, S. Szilner, D. Bazzacco, M. Bowry, A. Bracco, B. Bruyneel, F. C. L. Crespi, G. de Angelis, P. Désesquelles, J. Eberth, E. Farnea, E. Fioretto, A. Gadea, K. Geibel, A. Gengelbach *et al.*, *Phys. Rev. C* **92**, 024619 (2015).
- [33] E. M. Kozulin, V. I. Zagrebaev, G. N. Knyazheva, I. M. Itkis, K. V. Novikov, M. G. Itkis, S. N. Dmitriev, I. M. Harca, A. E. Bondarchenko, A. V. Karpov, V. V. Saiko, and E. Vardaci, *Phys. Rev. C* **96**, 064621 (2017).
- [34] T. Welsh, W. Loveland, R. Yanez, J. Barrett, E. McCutchan, A. Sonzogni, T. Johnson, S. Zhu, J. Greene, A. Ayangeakaa, M. Carpenter, T. Lauritsen, J. Harker, W. Walters, B. Amro, and P. Copp, *Phys. Lett. B* **771**, 119 (2017).
- [35] S. Wuenschel, K. Hagel, M. Barbui, J. Gauthier, X. G. Cao, R. Wada, E. J. Kim, Z. Majka, R. Płaneta, Z. Sosin, A. Wieloch, K. Zelga, S. Kowalski, K. Schmidt, C. Ma, G. Zhang, and J. B. Natowitz, *Phys. Rev. C* **97**, 064602 (2018).
- [36] V. V. Desai, W. Loveland, K. McCaleb, R. Yanez, G. Lane, S. S. Hota, M. W. Reed, H. Watanabe, S. Zhu, K. Auranen, A. D. Ayangeakaa, M. P. Carpenter, J. P. Greene, F. G. Kondev, D. Seweryniak, R. V. F. Janssens, and P. A. Copp, *Phys. Rev. C* **99**, 044604 (2019).
- [37] H. Imai and R. Ogul, *Nucl. Phys. A* **1014**, 122261 (2021).
- [38] K. Palli, G. A. Souliotis, T. Depastas, I. Dimitropoulos, O. Fasoula, S. Koulouris, M. Veselsky, S. J. Yennello, and A. Bonasera, *EPJ Web Conf.* **252**, 07002 (2021).
- [39] S. Gales, *Prog. Part. Nucl. Phys.* **59**, 22 (2007).
- [40] Y. Yano, *Nucl. Instrum. Methods Phys. Res. B* **261**, 1009 (2007).
- [41] M. Winkler, H. Geissel, H. Weick, B. Achenbach, K. H. Behr, D. Boutin, A. Brünle, M. Gleim, W. Hüller, C. Karagiannis, A. Kelic, B. Kindler, E. Kozlova, H. Leibrock, B. Lommel, G. Moritz, C. Mühlé, G. Münzenberg, C. Nociforo, W. Plass *et al.*, *Nucl. Instrum. Methods Phys. Res. B* **266**, 4183 (2008).
- [42] J. Yang, J. Xia, G. Xiao, H. Xu, H. Zhao, X. Zhou, X. Ma, Y. He, L. Ma, D. Gao, J. Meng, Z. Xu, R. Mao, W. Zhang, Y. Wang, L. Sun, Y. Yuan, P. Yuan, W. Zhan, J. Shi *et al.*, *Nucl. Instrum. Methods Phys. Res. B* **317**, 263 (2013).
- [43] A. Gade and B. M. Sherrill, *Phys. Scr.* **91**, 053003 (2016).
- [44] V. Zagrebaev and W. Greiner, *Phys. Rev. Lett.* **101**, 122701 (2008).
- [45] V. I. Zagrebaev and W. Greiner, *Phys. Rev. C* **83**, 044618 (2011).
- [46] V. I. Zagrebaev and W. Greiner, *Phys. Rev. C* **87**, 034608 (2013).
- [47] V. V. Saiko and A. V. Karpov, *Phys. Rev. C* **99**, 014613 (2019).
- [48] V. V. Volkov, *Phys. Rep.* **44**, 93 (1978).
- [49] G. Adamian, N. Antonenko, R. Jolos, and W. Scheid, *Nucl. Phys. A* **619**, 241 (1997).
- [50] G. G. Adamian, N. V. Antonenko, S. M. Lukyanov, and Y. E. Penionzhkevich, *Phys. Rev. C* **78**, 024613 (2008).

- [51] G. G. Adamian, N. V. Antonenko, and D. Lacroix, *Phys. Rev. C* **82**, 064611 (2010).
- [52] M. H. Mun, G. G. Adamian, N. V. Antonenko, Y. Oh, and Y. Kim, *Phys. Rev. C* **89**, 034622 (2014).
- [53] M. H. Mun, K. Kwak, G. G. Adamian, and N. V. Antonenko, *Phys. Rev. C* **99**, 054627 (2019).
- [54] M. H. Mun, K. Kwak, G. G. Adamian, and N. V. Antonenko, *Phys. Rev. C* **101**, 044602 (2020).
- [55] Z. Q. Feng, *Phys. Rev. C* **95**, 024615 (2017).
- [56] X. J. Bao, *Phys. Rev. C* **102**, 054613 (2020).
- [57] L. Zhu, P. W. Wen, C. J. Lin, X. J. Bao, J. Su, C. Li, and C. C. Guo, *Phys. Rev. C* **97**, 044614 (2018).
- [58] L. Zhu, C. Li, J. Su, C. C. Guo, and W. Hua, *Phys. Lett. B* **791**, 20 (2019).
- [59] G. Zhang, C. A. T. Sokhna, Z. Liu, and F. S. Zhang, *Phys. Rev. C* **100**, 024613 (2019).
- [60] X. R. Zhang, G. Zhang, J. J. Li, S. H. Cheng, Z. Liu, and F. S. Zhang, *Phys. Rev. C* **103**, 024608 (2021).
- [61] A. Winther, *Nucl. Phys. A* **572**, 191 (1994).
- [62] A. Winther, *Nucl. Phys. A* **594**, 203 (1995).
- [63] R. Yanez and W. Loveland, *Phys. Rev. C* **91**, 044608 (2015).
- [64] S. Ayik, *Phys. Lett. B* **658**, 174 (2008).
- [65] K. Sekizawa and K. Yabana, *Phys. Rev. C* **88**, 014614 (2013).
- [66] K. Sekizawa and K. Yabana, *Phys. Rev. C* **93**, 054616 (2016).
- [67] S. Ayik, O. Yilmaz, B. Yilmaz, A. S. Umar, A. Gokalp, G. Turan, and D. Lacroix, *Phys. Rev. C* **91**, 054601 (2015).
- [68] S. Ayik, B. Yilmaz, O. Yilmaz, and A. S. Umar, *Phys. Rev. C* **97**, 054618 (2018).
- [69] S. Ayik, O. Yilmaz, B. Yilmaz, and A. S. Umar, *Phys. Rev. C* **100**, 044614 (2019).
- [70] J. Tian, X. Wu, K. Zhao, Y. Zhang, and Z. Li, *Phys. Rev. C* **77**, 064603 (2008).
- [71] K. Zhao, Z. Li, N. Wang, Y. Zhang, Q. Li, Y. Wang, and X. Wu, *Phys. Rev. C* **92**, 024613 (2015).
- [72] C. Li, F. Zhang, J. Li, L. Zhu, J. Tian, N. Wang, and F. S. Zhang, *Phys. Rev. C* **93**, 014618 (2016).
- [73] C. Li, P. Wen, J. Li, G. Zhang, B. Li, X. Xu, Z. Liu, S. Zhu, and F. S. Zhang, *Phys. Lett. B* **776**, 278 (2018).
- [74] C. Li, J. Tian, and F.-S. Zhang, *Phys. Lett. B* **809**, 135697 (2020).
- [75] L. Corradi, G. Pollarolo, and S. Szilner, *J. Phys. G* **36**, 113101 (2009).
- [76] J. V. Kratz, W. Loveland, and K. J. Moody, *Nucl. Phys. A* **944**, 117 (2015).
- [77] F. S. Zhang, C. Li, L. Zhu, and P. W. Wen, *Front. Phys.* **13**, 132113 (2018).
- [78] L. Zhu, C. Li, C. C. Guo, J. Su, P. W. Wen, G. Zhang, and F. S. Zhang, *Int. J. Mod. Phys. E* **29**, 2030004 (2020).
- [79] W. D. Loveland, *Front. Phys.* **7**, 23 (2019).
- [80] G. G. Adamian, N. V. Antonenko, A. Diaz-Torres, and S. Heinz, *Eur. Phys. J. A* **56**, 1 (2020).
- [81] K. Washiyama and K. Sekizawa, *Front. Phys.* **8**, 93 (2020).
- [82] Z. Q. Feng, G. M. Jin, J. Q. Li, and W. Scheid, *Phys. Rev. C* **76**, 044606 (2007).
- [83] C. Y. Wong, *Phys. Rev. Lett.* **31**, 766 (1973).
- [84] L. Zhu, F. S. Zhang, P. W. Wen, J. Su, and W. J. Xie, *Phys. Rev. C* **96**, 024606 (2017).
- [85] S. Ayik, B. Schürmann, and W. Nörenberg, *Z. Phys. A* **277**, 299 (1976).
- [86] J. J. Li, G. Zhang, X. R. Zhang, Y. H. Zhang, Z. Liu, and F. S. Zhang, *J. Phys. G: Nucl. Part. Phys.* **49**, 025106 (2022).
- [87] G. Wolschin and W. Nörenberg, *Z. Phys. A* **284**, 209 (1978).
- [88] R. J. Charity, *Phys. Rev. C* **82**, 014610 (2010).
- [89] D. Mancusi, R. J. Charity, and J. Cugnon, *Phys. Rev. C* **82**, 044610 (2010).
- [90] R. Bass, *Phys. Rev. Lett.* **39**, 265 (1977).